AIAA SciTech Forum
8-12 January 2024, Orlando, FL
AIAA SCITECH 2024 Forum

10.2514/6.2024-1793

Process modeling of the Fused Filament Fabrication of semi-crystalline thermoplastics

Manish H. Nagaraj* and Marianna Maiaru†
Department of Mechanical Engineering, University of Massachusetts Lowell, 01854 MA.

The present works extends previous efforts in the process modeling of Fused Filament Fabrication by incorporating the effects of crystallinity evolution within the thermoplastic material. Material crystallinity is highly dependent on the process-based thermal history, and the resulting crystalline state after fabrication determines the part's mechanical response. The proposed computational framework employs higher-order structural theories derived from the Carrera Unified Formulation, and the element activation approach simulates the material deposition process. A modified version of the Velisaris and Seferis crystallization kinetics model is used to determine the evolving crystallinity under non-isothermal processing conditions. A set of numerical assessments is presented to verify the semi-crystalline kinetics model within the FFF process framework, and a good agreement between predicted results and available test data validates the model.

I. Nomenclature

FFF	=	Fused Filament Fabrication
FEM	=	Finite Element Method
CUF	=	Carrera unified Formulation
X	=	Crystallinity
$p = \{w_i, C_{i1}, C_{i2}, C_{i3}, T_{add,i}, T_{m,i}\}$	=	Model fitting parameters

II. Introduction

Fused Filament Fabrication (FFF) is an additive manufacturing process involving the deposition of semi-molten thermoplastic material along a pre-defined path, in a layer-by-layer manner, to achieve the fabrication of the required 3D geometry. This processing technique, commonly referred to as 3D-printing, has become very popular over the past two decades due to its capability in processing complex 3D parts which may not be otherwise possible with conventional manufacturing methods. Due to the nature of the manufacturing technique, FFF involves a highly variable thermal state, i.e., deposition at a high temperature and subsequent cooldown based on ambient conditions. This introduces thermal gradients within the manufactured part resulting in the development of residual stresses and deformations [1].

The dynamic thermal state of the part during its processing can also influence material properties and its response. In particular, semi-crystalline thermoplastics are highly susceptible to processing conditions. The thermal state of the material, as well as the rate of temperature change with time, influences the nucleation and growth of crystals within the polymer microstructure [2]. The degree of crystallinity during and at the end of processing determines the mechanical properties of the deposited material, and hence the dimensional accuracy (due to warpage) and mechanical performance of the fabricated part [3]. It is therefore important to consider the effect of the processing conditions on the material state for the FFF of semi-crystalline thermoplastics.

Process modeling has emerged as a popular approach to establish favorable manufacturing conditions by virtually identifying critical parameters which affect part quality, and has been extensively applied to thermoset composite manufacturing [4–6]. Similar efforts have been made in recent years to develop process models for additive manufacturing [1]. The present work proposes a novel computational framework for FFF process modeling [7–9], and extends previous efforts in the thermal modeling of the FFF process by including the effects of processing conditions on the crystallinity evolution within the thermoplastic material. The framework is based on higher-order finite elements developed using

*Postdoctoral Research Associate
†Associate Professor (AIAA member: Technical Committee - Materials)

structural theories derived from the Carrera Unified Formulation (CUF) [10]. This approach allows for the development of a fully 3D numerical model, and hence a 3D solution, at reduced computational costs when compared to traditional finite element analysis (FEA) [11–13]. This work is part of current research efforts in investigating the capabilities of CUF models in the process modeling of thermoset and thermoplastic material systems [5, 7, 8].

III. Computational Framework

A. Structural Modeling

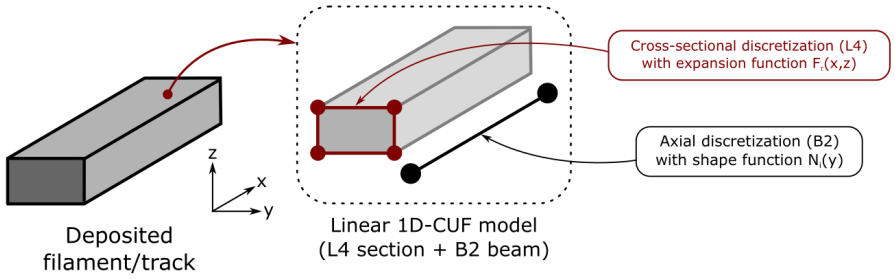

Fig. 1 Modeling of FFF in 1D-CUF.

The process modeling framework is developed using higher-order structural theories dervied via the Carrera Unified Formulation, and implemented in the form of finite elements. The present work considers the 1D CUF approach, wherein the interpolative capabilities of standard 1D finite elements is enriched by additional 2D functions, termed as expansion functions (F_τ), which describe the cross-sectional domain. This approach, in the context of FFF process modeling, is schematically shown in Fig. 1. The displacement field is formulated as

$$\mathbf{u} = F_\tau(x,z)\mathbf{u}_\tau(y),\ \tau = 1,2,...,M \tag{1}$$

where u_τ are the generalized displacements and F_τ is the 2D expansion function with M terms. Lagrange polynomials have been considered in the present work as F_τ, and allows for an explicit representation of the cross-sectional geometry, as seen in Fig. 1. The use of Lagrange polynomial-based expansion functions results in a Component-Wise modeling approach [14]. Further details on CUF structural modeling can be found in [10].

B. Additive Manufacturing Simulation

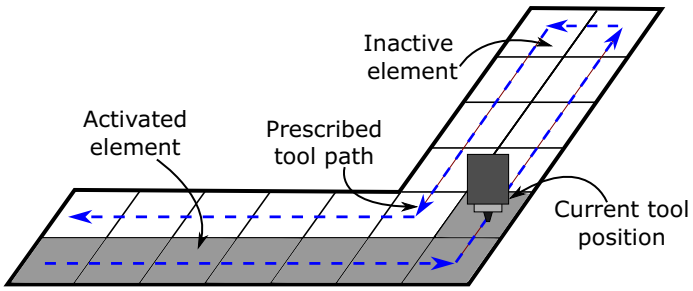

Fig. 2 2D schematic representation of the element activation strategy to model material deposition.

During the FFF process, the continuous deposition of material along the prescribed tool travel path results in an evolution of the structural domain as a function of time. This evolution is modeled in the numerical framework using the element activation strategy, schematically shown in Fig. 2. In this approach, a model of the full structure is developed and all elements are initially set to be inactive, i.e., they do not transmit loads. Within a time-step of the process simulation, the current tool position is evaluated from input data such as tool path and print velocity. The elements intersected during the incremental tool travel between consecutive time-steps are then activated, i.e. the elements are

capable of transmitting loads, and represent the deposition of material within the time-step. This is an important aspect of modeling AM processes, since the continuous evolution of the part domain leads to a changing volume and external surface area, shown schematically in Fig. 3. Accurately estimating these values is essential to quantify the heat transfer from the part due to thermal transport mechanisms such as conduction, convection and radiation (see Fig. 3). This is evaluated within a transient thermal analysis of the process model to obtain the thermal history of the part during print. Further details of FFF thermal modeling using the proposed framework is found in [7, 8].

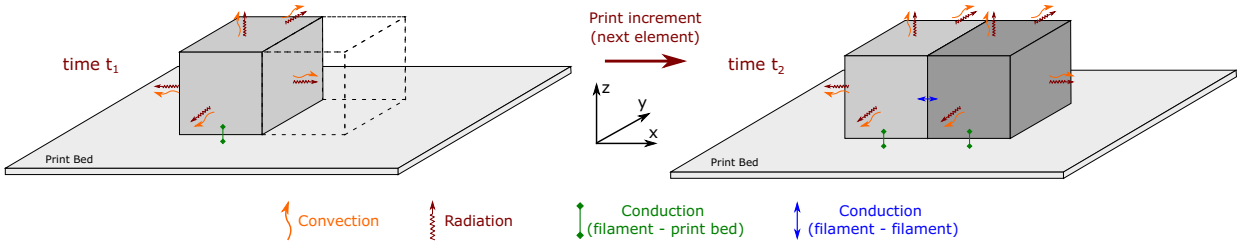

Fig. 3 Evolution of structure and heat transfer mechanisms due to material deposition.

C. Crystallization Kinetics

The crystallization kinetics model considered in the present study is based on the works of Brenken [15], and is a modified version of the Velisaris and Seferis model [16]. Following the model formulation, the degree of crystallinity X is evaluated as a function of the processing conditions as

$$X(t,T,p) = X_\infty[w_1 F_1(t,T) + w_2 F_2(t,T)] \tag{2}$$

with

$$F_i(t,T) = 1 - exp\left[-C_{i1}\int_0^t T \cdot exp\left\{\frac{-C_{i2}}{T - T_g + T_{add,i}} - \frac{C_{i3}}{T(T_{m,i} - T)^2}\right\} n_i \tau^{n_i - 1} d\tau\right] \; ; \; i = 1,2 \tag{3}$$

where X_∞ is the maximum crystalline volume fraction, w_i represents the weight fraction of mechanism-i, t and T are the process time and temperature, respectively. The Avrami exponent is denoted by n, and $p = \{w_i, C_{i1}, C_{i2}, C_{i3}, T_{add,i}, T_{m,i}\}$ represents the set of model fitting parameters obtained using material characterization data. The index $i = 1,2$ represents two mechanisms driving the kinetics of crystallization. The incremental form of Eq. (2), for a time increment Δt can be obtained by applying the midpoint rule as follows

$$\Delta I_i \cong C_{i1} T_M \, exp\left\{\frac{-C_{i2}}{T_M - T_g + T_{add,i}} - \frac{C_{i3}}{T_M (T_{m,i} - T_M)^2}\right\} n_i t_M^{n_i - 1} \Delta t \; ; \; i = 1,2 \tag{4}$$

where T_M and t_M are respectively the mid-interval temperature and time. The crystallinity can then be evaluated as

$$X = X_\infty \left\{ w_1 \left[1 - exp\left(\sum_{j=1}^{n} \Delta I_{1,j}\right)\right] + (1 - w_1)\left[1 - exp\left(\sum_{j=1}^{n} \Delta I_{2,j}\right)\right]\right\} \tag{5}$$

IV. Numerical Assessment

A. Crystallization kinetics

The crystallization kinetics model discussed in Section III.C has been implemented within the FFF process modeling framework, and a set of numerical assessments for verification are presented herein. The material system considered is polyphenylene sulfide (PPS) reinforced with 50% carbon fiber (CF), hereinafter referred to as PPS-50, and has been previously characterized by Brenken [15]. The fitted kinetics model parameters are listed in Table 1.

The verification study evaluates the evolution of crystallinity under a cooldown of the material from an initial temperature of 330 $^\circ C$, at a prescribed constant cooldown rate. The crystallinity evolution predicted by the process model is plotted in Fig. 4 for two cooldown rates, 100 and 130 $^\circ C/min$, respectively. Reference model predictions

Table 1 Crystallization kinetics parameters for the CF reinforced PPS material system [15].

Parameter	Mechanism-1	Mechanism-2
w_i	0.765	0.235
n_i	3	2
$C_{i1}[s^{-n}K^{-1}]$	1.16e11	4.733e13
$C_{i2}[K]$	1.19e4	1.045e3
$C_{i3}[K^3]$	3.27e7	2.387e8
$T_{m,i}[K]$	577.51	599.74
$T_{add,i}[K]$	218.70	1.07

and experimental data from [15] has also been overlaid for comparison. The perfect agreement with reference model predictions verifies the implementation within the present process modeling framework, while the general agreement with experimental data points validates the kinetics model.

The capability of the kinetics model in predicting the maximum crystal volume fraction at different cooldown rates is then investigated, and has been plotted in Fig. 5. Available reference data from [15] has also been reported for comparison. The agreement between model predictions and experimental data at varying cooldown rates, especially for temperature ranges typically associated with FFF for the considered material system, indicates the suitability of this crystallization kinetics model in predicting crystallinity evolution during the FFF process modeling of semi-crystalline thermoplastics.

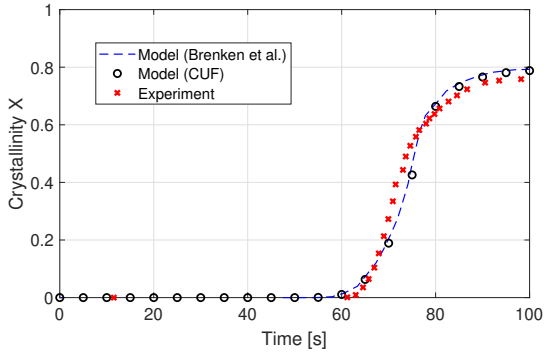

(a) 100 $^\circ C/min$

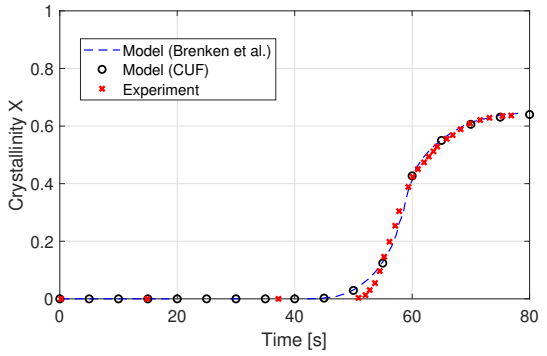

(b) 130 $^\circ C/min$

Fig. 4 Crystallinity evolution under cooldown from an initial temperature (330 $^\circ C$) at a constant rate. Reference model predictions and experimental data from [15].

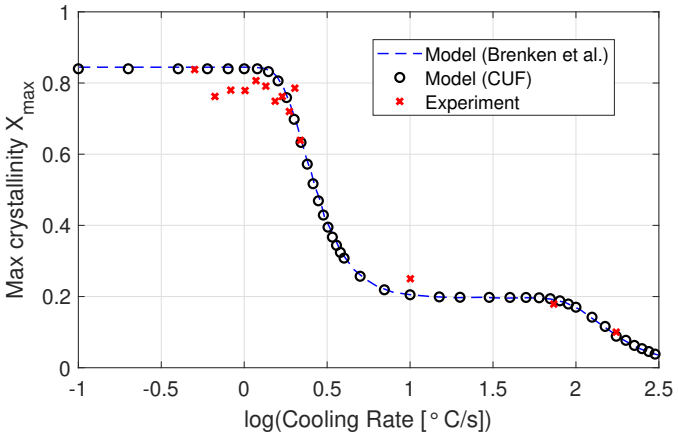

Fig. 5 Model prediction of maximum crystallinity as a function of cooling rate with experimental observations from [15] for comparison.

Table 2 FFF process parameters for the [0/90] cross-ply laminate [15].

Print velocity $[mm/s]$	$T_{dep}[^\circ C]$	$T_{bed}[^\circ C]$	$T_{amb}[^\circ C]$	$h[W/m^2K]$	$Emissivity[-]$
25	300	200	25	30	0.97

B. FFF of a [0/90] laminate

This section presents the FFF process simulation of a [0/90] cross-ply laminate printed using the PPS-50 composite material system, as described in [15]. The print geometry is a 125 mm square plate with a total thickness of 2.6 mm. The extruded track dimension is 4.7 mm wide with a height of 1.3 mm. The print parameters are listed in Table 2, and a print velocity of 25 mm/s has been assumed for the present analysis. The temperature-dependent material properties are listed in Table 3.

The print domain has been modeled in the present FFF framework using a single L4 section element to represent the cross-section of the deposited track, and 26 B2 axial elements were used in the discretization along the x-axis (see Fig. 1). The temperature and crystallinity distribution at the end of the printing process, for Layer-2 of the cross-ply laminate, has been visualized in Fig. 6. It is seen from the figure that newly deposited material is initially amorphous as a consequence of the deposition temperature, and crystallinity develops as the material cools down to equilibrate with the ambient conditions. The maximum crystallinity in the printed laminate is shown to be 0.84, and is in perfect agreement with the experimentally and numerically obtained maximum crystallinity values for a range of cooling rates, as shown in Fig. 5.

Table 3 Temperature-dependent material properties of PPS-50[15].

Temperature $[^\circ C]$	Density $[\frac{g}{cm^3}]$	Specific heat $[\frac{J}{gK}]$
23.0	1.2623	0.9215
50.0	1.2623	0.9746
100.0	1.2623	1.1285
150.0	1.2623	1.2726
200.0	1.2623	1.4120
250.0	1.2623	1.5401

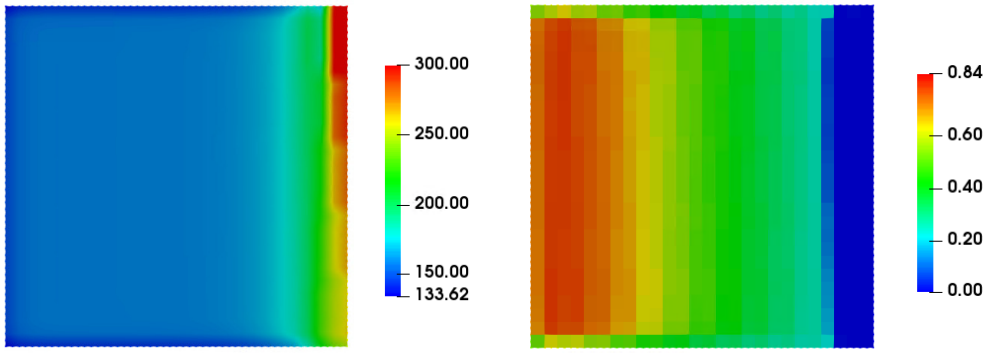

Fig. 6 (a) Temperature [°C], and (b) crystallinity distribution in Layer-2 of the [0/90] laminate at the end of the printing process.

V. Conclusion

A computational process modeling framework has been developed for FFF-based additive manufacturing, and incorporates a non-isothermal crystallization kinetics model to determine the development of the crystalline phase within the thermoplastic as a function of the FFF processing conditions. Verification assessments are performed by evaluating the crystallinity evolution of the thermoplastic under prescribed cooling rates, while a good agreement with available experimental data validates the considered crystallization kinetics model. The FFF of a [0/90] cross-ply laminate is also simulated via a transient thermal analysis, and the resulting thermal profile is used to evaluate the process-induced semi-crystalline state in the printed part.

Future works will extend the process model to incorporate a thermo-mechanical analysis, which would enable process-induced warpage prediction due to the development of thermal- and crystallization shrinkage- induced strains in the printed part.

Acknowledgments

This material is based upon work supported by the National Science Foundation under grant number IIP-1822147 (Phase I IUCRC at University of Massachusetts Lowell: Center for Science of Heterogeneous Additive Printing of 3D Materials (SHAP3D)) and from the SHAP3D I/UCRC Members, and National Science Foundation CAREER Award #2145387. Any opinions, findings, and conclusions or recommendations expressed in this material are those of the author(s) and do not necessarily reflect the views of the National Science Foundation or the sponsors.

References

[1] Cattenone, A., Morganti, S., Alaimo, G., and Auricchio, F., "Finite element analysis of additive manufacturing based on fused deposition modeling: distortions prediction and comparison with experimental data," *Journal of Manufacturing Science and Engineering*, Vol. 141, No. 1, 2019.

[2] Nakamura, K., Watanabe, T., Katayama, K., and Amano, T., "Some aspects of nonisothermal crystallization of polymers. I. Relationship between crystallization temperature, crystallinity, and cooling conditions," *Journal of Applied Polymer Science*, Vol. 16, No. 5, 1972, pp. 1077–1091.

[3] Glomsaker, T., Larsen, Å., Andreassen, E., and Ommundsen, E., "Experimental and numerical investigation of warpage of semicrystalline polymers in rotational molding," *Polymer Engineering & Science*, Vol. 45, No. 7, 2005, pp. 945–952.

[4] Nagaraj, M., and Maiaru, M., "Micro-Scale Process Modeling and Evaluation of Curing-Induced Residual Stresses in Fiber-Reinforced Polymers Using Higher-Order FE Models," *PROCEEDINGS OF THE AMERICAN SOCIETY FOR COMPOSITES-THIRTY-SEVENTH TECHNICAL CONFERENCE*, 2022.

[5] Nagaraj, M. H., and Maiaru, M., "Micro-scale process modeling and residual stress prediction in fiber-reinforced polymers using refined structural models," *arXiv preprint arXiv:2212.06792*, 2022.

[6] Nagaraj, M., and Maiaru, M., "Curing-Induced Residual Stress and Strain in Thermoset Composites," *ChemRxiv*, 2023.

[7] Nagaraj, M., Hansen, C. J., and Maiaru, M., "Rapid thermal analysis of the Fused Filament Fabrication process," *AIAA SCITECH 2023 Forum*, 2023, p. 0316.

[8] Nagaraj, M., and Maiaru, M., "A novel higher-order finite element framework for the process modeling of material extrusion additive manufacturing," *Additive Manufacturing*, Vol. 76, 2023, p. 103759.

[9] Nagaraj, M., Hansen, C. J., and Maiaru, M., "Process modeling and distortion prediction of Fused Filament Fabrication using higher-order finite elements," *PROCEEDINGS OF THE AMERICAN SOCIETY FOR COMPOSITES-THIRTY-EIGHTH TECHNICAL CONFERENCE*, 2023.

[10] Carrera, E., Cinefra, M., Petrolo, M., and Zappino, E., *Finite element analysis of structures through unified formulation*, John Wiley & Sons, 2014.

[11] Nagaraj, M., Kaleel, I., Carrera, E., and Petrolo, M., "Contact analysis of laminated structures including transverse shear and stretching," *European Journal of Mechanics-A/Solids*, Vol. 80, 2020, p. 103899.

[12] Nagaraj, M., Petrolo, M., and Carrera, E., "A global–local approach for progressive damage analysis of fiber-reinforced composite laminates," *Thin-Walled Structures*, Vol. 169, 2021, p. 108343.

[13] Nagaraj, M., Carrera, E., and Petrolo, M., "A global–local approach to the high-fidelity impact analysis of composite structures based on node-dependent kinematics," *Composite Structures*, Vol. 304, 2023, p. 116307.

[14] Carrera, E., Maiarú, M., and Petrolo, M., "Component-wise analysis of laminated anisotropic composites," *International Journal of Solids and Structures*, Vol. 49, No. 13, 2012, pp. 1839–1851.

[15] Brenken, B., "Extrusion deposition additive manufacturing of fiber reinforced semi-crystalline polymers," Ph.D. thesis, Purdue University, 2017.

[16] Velisaris, C. N., and Seferis, J. C., "Crystallization kinetics of polyetheretherketone (PEEK) matrices," *Polymer Engineering & Science*, Vol. 26, No. 22, 1986, pp. 1574–1581.